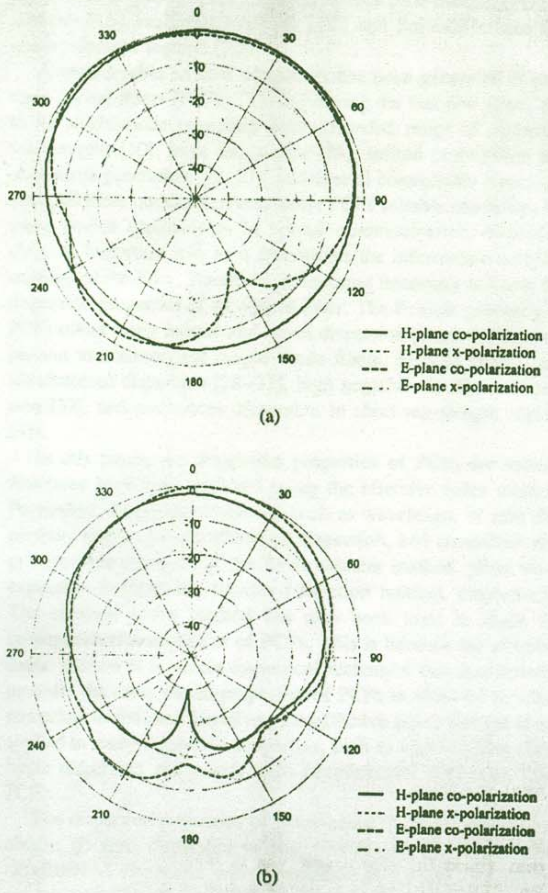

Figure 3 Measured radiation patterns at (a) 1 GHz and (b) 1.81 GHz

the antenna gain is measured from 0.65 GHz to 2.35 GHz at 0°. A maximum gain of 3–4 dBi can be obtained for both bands.

4. CONCLUSION

A dual-band dual shorted-patch antenna, proximity-fed by a combined L- and T-probe feed structure, has been reported experimentally. The bandwidth of the antenna is so wide that it can meet the bandwidth requirements of several operating systems for mobile communications, such as CDMA800, GSM900, GSM1900, and 3G. Thus, this antenna can be used as an antenna for indoor communication systems.

ACKNOWLEDGMENTS

This project is supported by the Research Grant Council of Hong Kong through the CERG project CityU 1167\99E.

REFERENCES

1. S. Pinhas and S. Shtrikman, Comparison between computed and measured bandwidth of quarter-wave microstrip radiators, IEEE Trans Antennas Propagat AP-36 (1988), 1615–1616.
2. R.B. Waterhouse, Small microstrip patch antenna, Electron Lett 31 (1995), 604–605.
3. L. Zaid, G. Kossiavas, J.Y. Dauvignac, J. Cazajous, and A. Papiernik, Dual-frequency and broad-band antennas with stacked quarter wavelength elements, IEEE Trans AP-47 (1999), 654–660.
4. Y.X. Guo, K.M. Luk, and K.F. Lee, Dual-band slot-loaded short-circuited patch antenna, Electron Lett 36 (2000), 289–291.
5. K.M. Luk, C.L. Mak, Y.L. Chow, and K.F. Lee, A novel broadband microstrip patch antenna, Electron Lett 34 (1998), 1442–1443.
6. C.L. Mak, K.F. Lee, and K.M. Luk, Broadband patch antenna with a T-shaped probe, Microwaves, Antennas and Propagation, IEE Proceedings 2 (2000), 73–76.
7. K.M. Luk, C.H. Lai, and K.F. Lee, Wideband L-probe-feed patch antenna with dual-band operation for GSM/PCS base stations, Electron Lett 35 (1999), 1442–1443.
8. Y.X. Guo, K.M. Luk, and K.F. Lee, L-probe proximity-fed short-circuited patch antennas, Electron Lett 35 (1999), 2069–2070.

DISPERSION PROPERTIES OF PHOTONIC CRYSTAL FIBERS

R. K. Sinha and Shailendra K. Varshney
Department of Applied Physics
Delhi College of Engineering
Faculty of Technology
University of Delhi
Bawana Road, Delhi-110 042, India

Received 2 October 2002

ABSTRACT: *The dispersion properties of silica-based photonic crystal fibers (PCFs) are analyzed to obtain: (i) zero dispersion at any wavelength, (ii) nearly zero ultraflattened dispersion, and (iii) a very high negative chromatic dispersion for various designs of PCFs. The influence of normalized air hole size on zero dispersion wavelength is also reported.* © 2003 Wiley Periodicals, Inc. Microwave Opt Technol Lett 37: 129–132, 2003; Published online in Wiley InterScience (www.interscience.wiley.com). DOI 10.1002/mop.10845

Key words: *photonic crystal fiber; effective index method; zero dispersion wavelength; normalized air hole size; pitch*

1. INTRODUCTION

The requirements of large bandwidth and miniaturization of circuits leads to the development of periodic dielectric structures that exhibit band gaps in the frequency spectrum. These structures are commonly known as photonic crystals or photonic bandgap materials in the literature. They have captured worldwide R&D interest because of their manipulation and localization of light [1–7] in photonic bandgap. Photonic crystals are artificial dielectric structures with the property of rejecting a frequency band of electromagnetic waves while transmitting frequencies outside the bandgap. Such crystals are the optical analog of semiconductors, because their periodic dielectric structure produces a photonic bandgap. The presence of photonic bandgap opens the possibility for a variety of applications, ranging from optical communication and integrated photonics to quantum information science. The introduction of defects in photonic crystals makes them useful for various purposes. The line defect, or removal of the air-hole column, gives rise to the confinement of light in the defect region. This property of photonic crystals is utilized in the development of Photonic Crystal Fibers [8], where the light is caged in the transverse plane and allowed to propagate in a third dimension, that is, out of the PCF plane [9]. Since the first experimental demonstration of photonic crystal fiber in 1996 [8], many modeling techniques have been applied to study its propagation characteristics, which include the effective index method [10, 11], plane-wave expansion method [12–14], localized function method [15–16],

finite element method [17], finite-difference time-domain (FDTD) methods [18], multipole methods [19], and finite-difference frequency-domain method [20].

A considerable amount of interest has been generated in photonic crystal fibers (PCFs) [21–24] during the last few years, due to its single-mode operation over extended range of operating wavelengths [10], large mode area [25], soliton propagation and continuum generation [26, 27], and overall controllable dispersion [16]. All these unusual features make PCFs suitable candidates for many device applications. In optical communication, dispersion plays an important role as it determines the information carrying capacity of the fiber. Therefore, it becomes necessary to know the dispersion properties of an optical fiber. The flexible geometry of PCFs offers many unique and novel dispersion properties in comparison to conventional single mode fibers, such as nearly zero ultraflattened dispersion [28–31], high negative chromatic dispersion [32], and anomalous dispersion in short-wavelength regime [33].

In this paper, the dispersion properties of PCFs for various structures have been analyzed using the effective index method. Previously, dispersion properties such as wavelength of zero dispersion, nearly zero ultraflattened dispersion, and anomalous dispersion were obtained by the finite element method, plane wave expansion method, and localized function method, respectively. The effective index method has also been used to study the propagation characteristics of PCFs. This is because the effective index method is a simple numerical technique that qualitatively provides the same modal properties of PCFs as obtained by other numerical techniques. However, the effective index method is not applied to study dispersion properties, such as high negative chromatic dispersion and nearly zero ultraflattened dispersion from PCF.

The dispersion properties of silica-based PCFs are analyzed to obtain: (i) zero dispersion at any wavelength, (ii) nearly zero ultraflattened dispersion with a variation of (+0.05, −0.25) ps/nm-km, and (iii) a very high negative chromatic dispersion for various designs of PCFs, using the effective index method. It is shown that a wavelength of zero dispersion can be altered to any value simply by changing the air hole size or separation between them. Nearly zero ultraflattened dispersion response from PCF has been achieved within wavelength range of 1.3 μm to 1.7 μm. Furthermore, a very high negative dispersion is found in PCFs of different core sizes. In addition, the negative dispersion of such a high value is also obtained from single-mode fiber with dual asymmetric and symmetric core [34], however, this fiber employs doped silica in its core. In the case of PCF, single material—pure silica—is used as a core and air holes are used as cladding in the present analysis. To the best of our knowledge, such high values of negative dispersion, as well as nearly zero ultraflattened dispersion with a variation of (+0.05, −0.25) ps/nm-km from PCF, are not reported in the literature so far. Accordingly, it is expected that this analysis of the dispersion properties of PCFs may be helpful in the design and development of optical communication systems.

2. DISPERSION CALCULATION

The dispersion characteristics of PCF are investigated by taking into account the refractive index of pure silica by means of the Sellemier formula, while the index of air is assumed constant. The dispersion D is given as [35]:

$$D = -\frac{\lambda}{c}\frac{d^2 n_e}{d\lambda^2} \qquad (1)$$

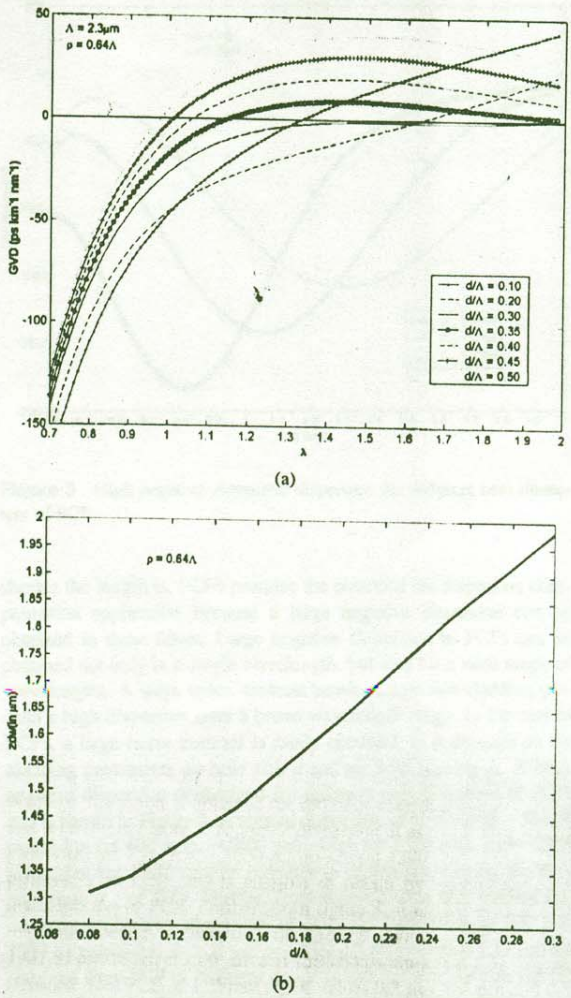

Figure 1 (a) Dispersion curves vs. wavelength for different normalized air hole size; (b) wavelength of zero dispersion against the normalized air hole size up to 0.30

where n_e represents the effective index of guided mode, which has been calculated as described in [12, 24] and λ (in μm) is the free-space wavelength.

2.1 Zero-Dispersion Wavelengths

To obtain zero dispersion wavelength (ZDW) for several structures of PCFs, a triangular photonic crystal lattice is assumed which has the following geometrical parameters, d as air hole diameter and Λ as air hole spacing (also referred to as pitch). Further, the core radius of the fiber is considered to be $\rho = 0.64\Lambda$ [17] instead of Λ as taken by Birks, et al. [10]. The dispersion (ps/nm-km) for different structures of PCF is obtained by use of Eq. 1 and shown in Figure 1(a). It is clear from Figure 1(a) that there is shift of zero dispersion wavelengths from the IR region of the spectrum towards the UV region, which is unattainable in conventional optical fiber. This means that one can design PCFs by choosing appropriate cladding parameters (namely, size of air hole d and pitch of the lattice Λ) to obtain a desired ZDW. This shift of zero dispersion wavelengths occurs mainly due to the wavelength-dependent effective cladding index. At short wavelength, the modal field re-

mains confined to the silica region, but at longer wavelengths the effective cladding index decreases. Thus, as we change the size of air hole d and separation between them Λ, ZDW can be altered to any value. This unusual dispersion characteristic of PCFs allows them to be used in non-linear fiber optics. It can also be seen from Figure 1(a) that these fibers have a great potential for use in dispersion compensation applications. Anomalous dispersion at smaller wavelengths arises due to the flexible geometry of the fiber, permittivity to solitons and ultrashort propagation [36], and generation of supercontinuum [27] in PCF. Variation of zero dispersion wavelengths with normalized air hole size is represented in Figure 1(b). It is clear from Figure 1(b) that the wavelength of zero dispersion increases as the air hole size increases.

2.2 *Nearly Zero Ultraflattened Dispersion*

From Figure 1(a) it is also obvious that one can design dispersion-flattened PCF over a broad range of wavelengths simply by tuning the cladding parameters. We have obtained the nearly zero ultra-flattened dispersion response with the following design parameters: air hole spacing $\Lambda = 2.3$ μm, diameter of air hole $d = 0.69$ μm, core diameter of 3 μm, and microstructured air-hole cladding in silica-based PCF. Figure 2 represents the variation of nearly zero ultraflattened dispersion from PCF with these design parameters, in the order of (+0.05, −0.25) ps/nm-km. This means that more ultraflattened response (around 10 times less) from PCF will be obtained, compared to the variation of (+0.5, −0.5) ps/nm-km reported by Ferrando, et al. [29]. This dispersion-flattened response of PCF can be utilized in dense-WDM (DWDM) based optical communication systems.

2.3 *High Negative Chromatic Dispersion*

Chromatic dispersion in single-mode fibers causes light pulses to spread, limiting the data transmission rate and length of optical-fiber links. To overcome these limits, various techniques are used to suppress the dispersion effects. Optical fibers presently installed in telecom links were designed for the transmission of 1300-nm light. However, they show dispersion (~20 ps/nm-km) at the currently preferred wavelength of 1550 nm. This large dispersion can be compensated by a short length of a special type of optical fibers, such as dispersion compensating fibers (DCFs), with a dispersion of opposite sign so that the net dispersion of two fibers in series becomes zero. The larger the negative dispersion of the compensating fiber, the shorter the length is. PCFs promise the potential for dispersion compensation application because a large negative dispersion can be obtained in these fibers. Large negative dispersion in PCFs can be obtained not only at a single wavelength, but also for a wide range of wavelengths. A large index contrast between core and cladding permits a high dispersion over a broad wavelength range. In the case of PCFs, a large index contrast is easily obtained, as it depends on the cladding parameters air hole size d and air hole spacing Λ. A large negative dispersion is obtained for different core diameters of PCFs and is shown in Figure 3. A normal dispersion of as much as −584.70 ps/nm-km (at 400 nm), −1600 ps/nm-km (at 1300 nm), and −1350 ps/nm-km (at 1550 nm) is possible to obtain by varying the core diameters d_{co} of PCF. Further, from figure 3, it is also evident that maximum negative dispersion of 2332.50 ps/nm-km at 0.8 μm, 1927.81 ps/nm-km at 1.06 μm and 1586.63 ps/nm-km at 1.31 μm are obtained from PCF of different d_{co} of values 0.3 μm, 0.4 μm and 0.5 μm respectively. These large values of negative dispersion could be used to compensate the anomalous dispersion of conventional single-mode fiber. This means that PCF can compensates the dispersion caused by standard single-mode fiber. Thus, large negative dispersion of PCFs make them useful candidates for use as dispersion compensating fibers in optical communication links.

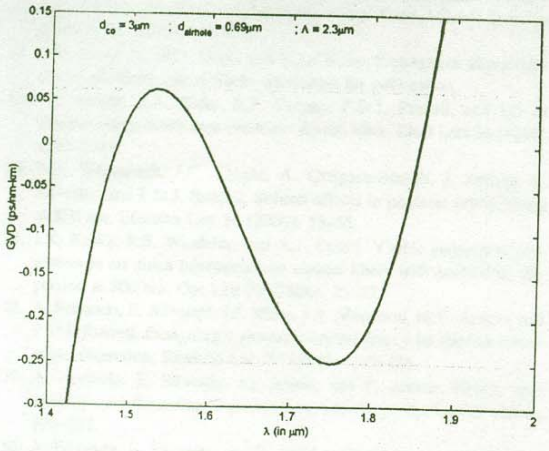

Figure 2 Nearly zero ultraflattened dispersion response in wavelength range of 1.3 μm to 1.7 μm

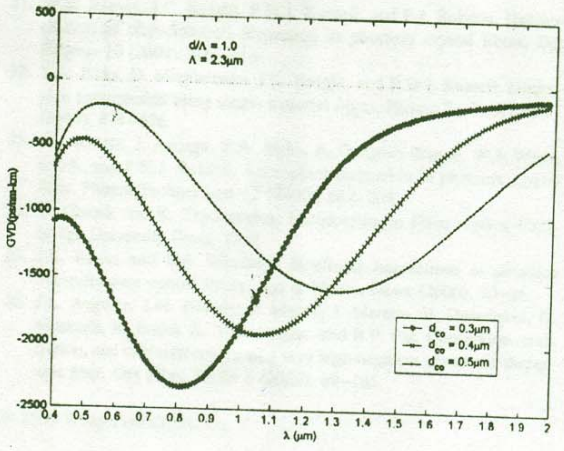

Figure 3 High negative chromatic dispersion for different core diameters of PCF

3. CONCLUSION

The dispersion properties of photonic crystal fibers (PCFs) was examined through scalar modal analysis. It was observed that the zero dispersion wavelengths for PCF can be engineered to any value by altering the size of air holes and separation between them. Nearly zero ultraflattened dispersion from PCFs will promote their application in DWDM communication systems, and the high negative chromatic dispersion in PCF will prove useful for dispersion-compensating devices.

REFERENCES

1. E. Yablonovitch, Inhibited spontaneous emission in solid state physics and electronics, Phys Rev Lett 58 (1987), 2059–2062.
2. S. John, Strong localization of photons in certain disordered dielectric superlattices, Phys Rev Lett 58 (1987), 2486–2489.
3. J.D. Joannopolous, R.D. Mead, and J.N. Winn, Photonic crystals: Molding the flow of light, Princeton University Press, Princeton, NJ, 1995.
4. K. Sakoda, Optical properties of photonic crystals, Springer, 2000.

5. See special issue on Photonic Crystal JOSA B 10 (1993); J Modern Optics 41 (1994).
6. See special issue on Photonic Crystal J Opt A: Pure Appl Optics 3 (2001).
7. See special issue on Photonic Crystal J Quantum Electronics 5 (2002).
8. J.C. Knight, T.A. Birks, P.St.J. Russell, and D.M. Atkin, All-silica single mode optical fiber with photonic crystal cladding, Opt Lett 21 (1996), 1547–1549.
9. A.A. Maradudin and A.R. McGurn, Off-angle dependence of photonic bandgap in a two-dimensional photonic crystals, J Modern Opt 41 (1994).
10. T.A. Birks, J.C. Knight, and P.St.J. Russell, Endlessly single-mode photonic crystal fiber, Opt Lett 22 (1997), 961–963.
11. J.C. Knight, T.A. Birks, P.St.J. Russell, and J.P. de Sandro, Properties of photonic crystal fiber and the effective index model, J Opt Soc Am A 15 (1998), 748–752.
12. A. Ferrando, E. Silvestre, J.J. Miret, P. Andres and M.V. Andres, Full-vector analysis of a realistic photonic crystal fiber, Opt Lett 24 (1999), 276–278.
13. A. Ferrando, E. Silvestre, J.J. Miret, and P. Andres, Vector description of higher order modes in photonic crystal fibers, J Opt Soc Am A 17 (2000), 1333–1340.
14. S.G. Johnson and J.D. Joannopoulos, Block-iterative frequency-domain methods for Maxwell's equations in a planewave basis, Opt Express 8 (2001), 173–190.
15. D. Mogilevstev, T.A. Birks, and P.St.J. Russell, Localized function method for modeling defect modes in 2-D photonic crystals, J Lightwave Technol 17 (1999), 2078–2081.
16. T.M. Monro, D.J. Richardson, N.G.R. Broderick, and P.J. Bennett, Holey Fibers: an efficient modal model, J Lightwave Technol 17 (1999), 1093–1101.
17. F. Brechet, J. Marcou, D. Pagnoux, and P. Roy, Complete analysis of the characteristics of propagation into photonic crystal fibers by the finite element method, Opt Fiber Technol 6 (2000), 181–191.
18. M. Qiu, Analysis of guided modes in photonic crystal fibers using the finite difference time domain method, Microwave Opt Technol Lett 30 (2001), 327–330.
19. T.P. White, R.C. McPhedran, C.M. de Sterke, L.C. Botten, and M.J. Steel, Confinement losses in microstructured optical fibers, Opt Lett 26 (2001), 1660–1662.
20. Z. Zhu and T.G. Brown, Full-vectorial finite-difference analysis of microstructured optical fibers, Opt Express 10 (2002), 853–864.
21. J. Broeng, D. Mogilevstev, S.E. Barkou, and A. Bjarklev, Photonic Crystal Fibers: A new class of optical waveguide, Opt Fiber Technol 5 (1999), 305–330.
22. J.C. Knight, T.A. Birks, R.F. Cregan, and P.St.J. Russell, Photonic crystals as optical fibers-Physics and applications, Opt Mater 11 (1998), 143–151.
23. R. Ghosh, A. Kumar, J.P. Meunier, and E. Marin, Modal characteristics of few-mode silica-based photonic crystal fibers, J Opt & Quantum Electron 32 (2000), 963–970.
24. S.K. Varshney, M.P. Singh, and R.K. Sinha, Propagation characteristics of photonic crystal fibers, submitted for publication.
25. J.C. Knight, T.A. Birks, R.F. Cregan, P.St.J. Russell, and J.P. de Sandro, Large mode area photonic crystal fiber, Elect Lett 34 (1998), 1347–1348.
26. W.J. Wadsworth, J.C. Knight, A. Ortigosa-Blanch, J. Arriaga, E. Silvestre, and P.St.J. Russell, Soliton effects in photonic crystal fibers at 850 nm, Electron Lett 36 (2000), 53–55.
27. J.K. Ranka, R.S. Windeler, and A.J. Stentz, Visible continuum generation in air silica microstructure optical fibers with anomalous dispersion at 800 nm, Opt Lett 25 (2000), 25–27.
28. A. Ferrando, E. Silvestre, J.J. Miret, J.A. Monsoriu, M.V. Andres, and P.St.J. Russell, Designing a photonic crystal fiber with flattened chromatic dispersion, Electron Lett 35 (1999), 325–326.
29. A. Ferrando, E. Silvestre, J.J. Miret, and P. Andres, Nearly zero ultraflattened dispersion in photonic crystal fibers, Opt Lett 25 (2000), 790–792.
30. A. Ferrando, E. Silvestre, and P. Andres, Designing the properties of dispersion-flattened photonic crystal fiber, Opt Express 9 (2000), 687–697.
31. W.H. Reeves, J.C. Knight, P.St.J. Russell, and P.J. Roberts, Demonstration of ultra-flattened dispersion in photonic crystal fibers, Opt Express 10 (2002), 609–613.
32. T.A. Birks, D. Mogilevstev, J.C. Knight, and P.St.J. Russell, Dispersion compression using single material fibers, Photon Technol Lett 11 (1999), 674–676.
33. J.C. Knight, J. Arriaga, T.A. Birks, A. Ortigosa-Blanch, W.J. Wadsworth, and P.St.J. Russell, Anomalous dispersion in photonic crystal fiber, Photon Technol Lett 12 (2000), 807–809.
34. A. Ghatak and K. Thyagarajan, Introduction to Fiber Optics, Cambridge University Press, 1999.
35. J.K. Ranka and R.S. Windeler, Nonlinear interactions in air-silica microstructure optical fibers, Opt & Photon News (2000), 20–25.
36. J.L. Auguste, J.M. Blondy, J. Maury, J. Marcou, B. Dussardier, G. Monnom, R. Jindal, K. Thyagarajan, and B.P. Pal, Conception, realization, and characterization of a very high negative chromatic dispersion fiber, Opt Fiber Techn 8 (2002), 89–105.

A TWO-STEP CALIBRATION TECHNIQUE FOR MEASURING S-PARAMETERS OF TRANSITIONAL STRUCTURES

Chao LI, Zhongxiang Shen, and Chol Look Law
Global Positioning Systems Centre
School of Electrical and Electronic Engineering
Nanyang Technological University
Nanyang Avenue, Singapore 639798

Received 1 October 2002

ABSTRACT: *A new two-step calibration technique to directly measure the scattering parameters of asymmetrical transitional structures is proposed in this article. This technique conducts two calibrations, each one of them for one type of the transition's two ports, and two error boxes associated with the transition measurement system can then be obtained, with which the transition's raw measured data can be corrected. Experimental studies have verified the validity of the formulation and the accuracy of the two-step calibration technique. The technique can be extensively used to measure the scattering parameters of transitional structures without resorting to constructing back-to-back test fixtures.*
 Microwave Opt Technol Lett 37: 132–135, 2003; Published online in Wiley InterScience (www.interscience.wiley.com). DOI 10.1002/mop.10846

Key words: *calibration techniques; transitions; vector network analyzer*

1. INTRODUCTION

It is well known that the systematic errors associated with a vector network analyzer (VNA) can be modeled by error port adapters. The widely-used eight-term error model was first proposed in [1]. To determine its error terms, a calibration procedure is required. Traditionally, coaxial short-open-load-through (SOLT) standards have been applied. However, it is difficult to realize these standards precisely in other media such as microstrip and coplanar waveguide (CPW). Hence, other calibration methods are desirable. Recently, TRL (thru, reflect, line) and TRM (thru, reflect, match) have become very popular [2–7] at very high frequency.

In order to measure the scattering parameters of transitional structures, a corresponding back-to-back transitional structure usually has to be fabricated, for example, grounded coplanar waveguide (GCPW)-to-microstrip transition [8], CPW-to-CPW transition [9], coaxial-to-microstrip transition [10], and waveguide-to-microstrip